

Application of Carbon Fibre Truss Technology to the Fuselage Structure of the SKYLON Spaceplane

RICHARD VARVILL AND ALAN BOND

Reaction Engines Ltd, D5 Culham Science Centre, Abingdon, Oxfordshire, OX14 3DB, UK.

A reusable SSTO spaceplane employing dual mode airbreathing/rocket engines, such as SKYLON, has a voluminous fuselage in order to accommodate the considerable quantities of hydrogen fuel needed for the ascent. The loading intensity which this fuselage has to withstand is relatively low due to the modest in-flight inertial accelerations coupled with the very low density of liquid hydrogen. Also the requirement to accommodate considerable temperature differentials between the internal cryogenic tankage and the aerodynamically heated outer skin of the vehicle imposes an additional design constraint that results in an optimum fuselage structural concept very different to conventional aircraft or rocket practice. Several different structural concepts exist for the primary loadbearing structure. This paper explores the design possibilities of the various types and explains why an independent near ambient temperature CFRP truss structure was selected for the SKYLON vehicle. The construction of such a truss structure, at a scale not witnessed since the days of the airship, poses a number of manufacturing and design difficulties. In particular the construction of the nodes and their attachment to the struts is considered to be a key issue. This paper describes the current design status of the overall truss geometry, strut construction and manufacturing route, and the final method of assembly. The results of a preliminary strut and node test programme are presented which give confidence that the design targets will eventually be met.

Keywords: Spaceplane design, SKYLON, CFRP space frame, fuselage structure.

1. Introduction

The SKYLON vehicle is a winged reusable SSTO spaceplane employing hybrid airbreathing rocket propulsion [1]. At a takeoff mass of 275 tonnes it is capable of placing a 12 tonne payload into an equatorial low Earth orbit. The vehicle is composed of a slender fuselage containing the propellant tankage and payload bay, with a relatively small delta wing positioned roughly midway along the fuselage carrying the engines housed within axisymmetric nacelles on the wingtips (Fig. 1). This configuration permits accurate pitch trimming of the vehicle for both ascent and re-entry whilst also resulting in an efficient structural arrangement. The wing area is relatively small for a vehicle of this size and represents an optimum balance between wing mass and overall vehicle drag which maximises vehicle payload. The vehicle fuselage is not blended into the wings as current re-entry vehicle practice, but rather is a completely separate component similar to aircraft wings. This approach enables a fuselage length to be chosen that minimises total aerodynamic drag (for good

airbreathing performance) whilst the circular cross section minimises tankage, aeroshell and insulation masses.

The payload bay is positioned over the wing to minimise centre of gravity movements regardless of whether the vehicle is returning with or without a payload during re-entry. This configuration also enables carry through wing spars to be placed underneath the payload bay and creates a natural void for undercarriage stowage. The liquid oxygen tankage is split into two ellipsoidal tanks either side of the payload bay, which ensures that the fuelled centre of gravity is in the correct position whilst minimising the fuselage bending moments. The remainder of the forward and aft fuselage is mostly filled with liquid hydrogen tankage.

The airbreathing ascent consumes approximately 41 tonnes of liquid hydrogen whilst the rocket ascent consumes a further 25 tonnes of hydrogen and 150 tonnes of liquid oxygen. The large consumption of liquid hydrogen compared to a purely rocket propelled vehicle results in a relatively voluminous fuse-

Revised version of Paper IAF-99-V.4.07, 50th International Astronautical Federation Congress, Amsterdam, Netherlands, October 1999.

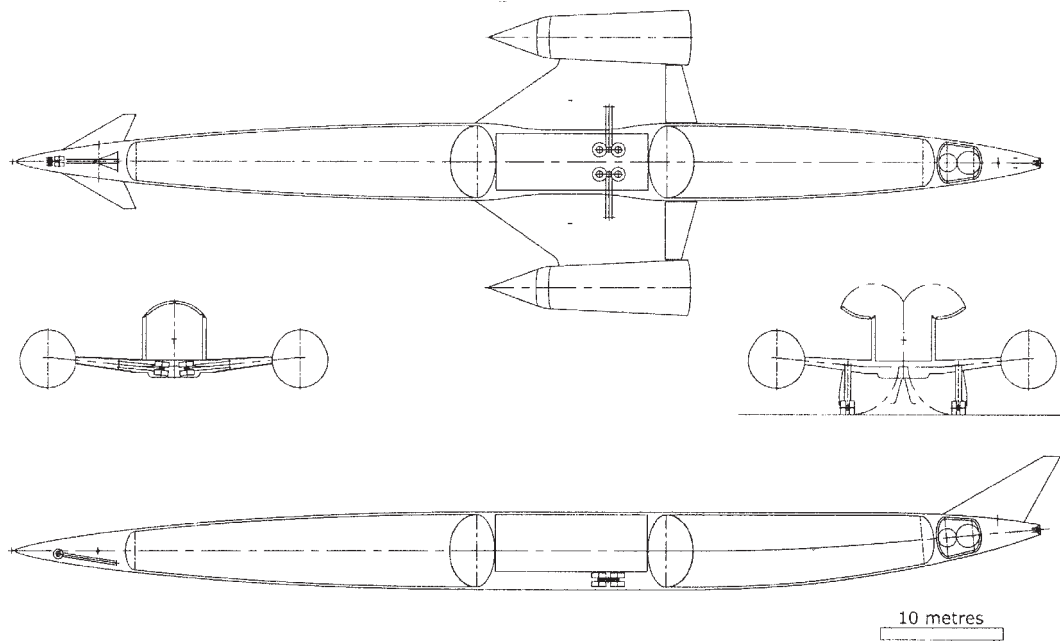


Fig. 1 SKYLON configuration C1.

lage which increases the fuselage surface area, drag and potentially mass. However it also reduces the ballistic coefficient during re-entry which enables beneficial design alterations to the aeroshell and thermal protection insulation (TPI) due to the reduced re-entry heat transfer rates. Consequently the structural mass penalty of increased hydrogen consumption is much smaller than simple parametric scaling might otherwise suggest.

In a similar manner it has been found that employing hydrogen fuel within the context of a spaceplanes unique operational environment results in a totally different optimum structure type compared to conventional aircraft practice. This is partly due to the smaller loading intensity induced by the very low density of liquid hydrogen (73.3 kg/m^3) in combination with the modest in-flight inertial accelerations (ascent maximum normal 2g). It is also due to the requirement to accommodate considerable temperature differentials between the internal cryogenic tankage (18 K) and the aerodynamically heated outer skin of the vehicle (1100 K). The structural solution chosen for SKYLON, and explored in this paper, is to introduce a tailored carbon fibre reinforced plastic truss structure into the gap between the cryogenic tankage and the hot aeroshell. This solution results in a diffuse structure that is able to sustain high stress levels whilst transferring modest loads over considerable distances without elastic collapse due to Euler instabilities.

Recently some of the technology issues relating to this type of structure have been explored as part of the 'Innovative Approaches to Composite Structures' programme funded under the IMI initiative by

the UK government [2]. Some of the results of this programme relating to truss structures are reported in the paper, especially focusing on those areas relating to the adhesive bonding of tubular joints.

2. Fuselage Structure Candidates

The fuselage can be regarded as a beam subject to aerodynamic and inertia loads along its length. The highest loads are in the vertical pitch plane (due to inertial and gust loads). However, significant lateral loads exist due to the aft fin and during yawed flight, whilst torsional moments are generated by the fin and the nosewheel. In addition the aerodynamic crossflow component due to the vehicle incidence attempts to distort the fuselage cross section out of round.

Three main structural design approaches exist, each of which has been proposed for various spaceplanes:

1) Structural aeroshell (Hot structure)

The aeroshell could be transformed into the main fuselage structure by stiffening the skin with frames and stringers in a similar manner to conventional aluminium airliner construction. This option is worth considering due to the relatively recent development of reinforced ceramics that have low density compared to the refractory metals. Apart from the practical difficulties of mounting the internal equipment and tankage from such a hot structure the main drawbacks of this approach are: a) Stiffened skins are relatively inefficient for lightly loaded structures, and b) The relatively poor stiffness/density and strength/density of reinforced ceramics compared to CFRP.

2) Structural tankage (Cold structure)

The main propellant tankage could be pressurised to the point that it can handle the maximum fuselage bending moment without buckling (similar to Atlas or Blue Streak). However since the bending moments on a horizontally launched lifting vehicle are greater than a vertically launched ballistic rocket, the pressure required to stabilise the tankage (≈ 2.5 bar) is much higher than the pressure required to satisfy pump NPSH limits (≈ 1 bar). Unfortunately the extra material needed to support the increased tank pressure is poorly distributed for an efficient beam and employed at a low effective stress level when resisting the fuselage bending moment. Also since the tankage does not extend the entire length of the fuselage, additional structure of a different type is required in the payload bay, nose and tailcone regions which is an extra complication. Finally the tankage must remain pressurised at all times otherwise the fuselage will collapse, leading to a rather delicate vehicle that is not easily handled on the ground.

3) Separate ambient structure

The remaining structural option is to introduce a separate tailored structure running down the length of the fuselage from which the tankage and the aeroshell are suspended. In reviewing the SKYLON fuselage construction it was realised that the novel insulation system had created a radial airgap at roughly ambient temperatures outside the tankage into which a cylindrical structure could be inserted (Fig. 2). This approach enabled the tank pressure to be reduced to the minimum governed by boost pump NPSH limits, and the aeroshell to be designed to carry the local aerodynamic pressure loading only. Also due to the relatively benign thermal environment, the structure could utilise the exceptional specific properties of carbon fibre reinforced plastics. Following a comparison of the structural alternatives this option was found to be the lightest solution for SKYLON.

3. Description of the Fuselage Structure

The structure must be capable of supporting compressive loads over considerable distances without buckling. Since the vehicle has a relatively low area loading (due to the hydrogen fuel and 2g stressing limit) and the relatively large section depth available (fuselage diameter 6.25 m), a very thin cylindrical shell is theoretically sufficient. However to satisfy elastic stability criteria whilst retaining high stress levels, the cylindrical shell must be locally condensed into small stable sections, frequently supported to satisfy global stability (i.e. a spaceframe). The actual truss structure is composed of ring frames (which support the aeroshell on radial posts) spaced at 300 mm intervals by shear diagonals (Fig. 3). Four longerons (roughly at the fuselage 45° points) carry the overall fuselage vertical and lateral bending moments and are tied into the truss structure at each frame. To avoid cut-outs and sudden changes in slope, the two upper longerons run just underneath the payload bay door sill whilst the two lower longerons run just above the wing carry-through, thereby avoiding the payload bay door and undercarriage well apertures (Fig. 4).

The design of the structure is dominated by stiffness rather than strength considerations at both a global and a local scale. For example, the forebody bending deflections are limited by the tank wall axial stress whilst the frame deflections are limited by the acceptable distortions of the fuselage cross section. Meanwhile, at a local level the design of the individual spaceframe members is controlled by Euler instability and local wall buckling. Therefore, to maximise the stress levels and hence

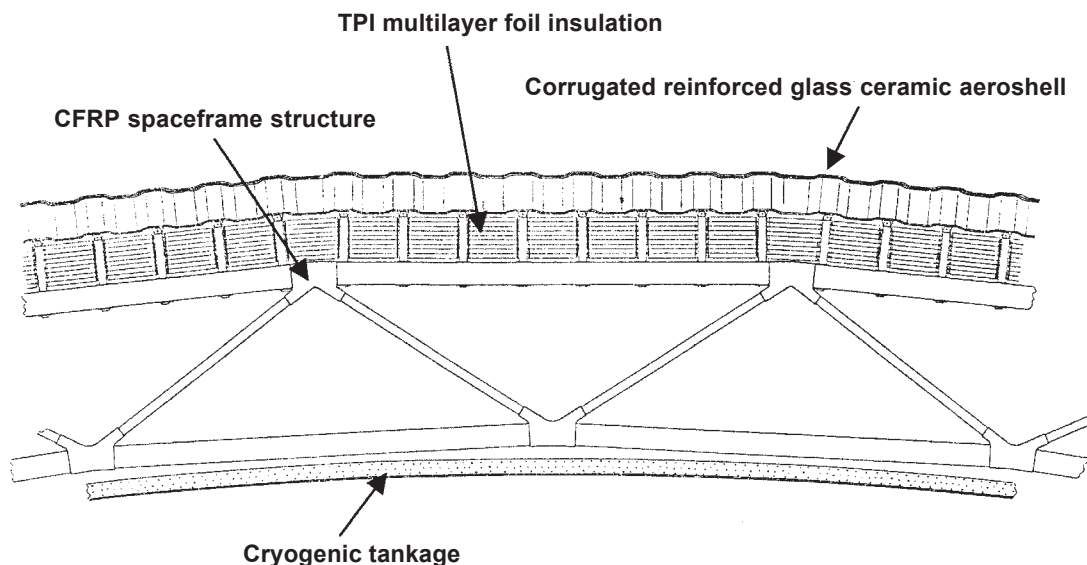


Fig. 2 Fuselage transverse section.

Fig. 3 Fuselage truss structure.

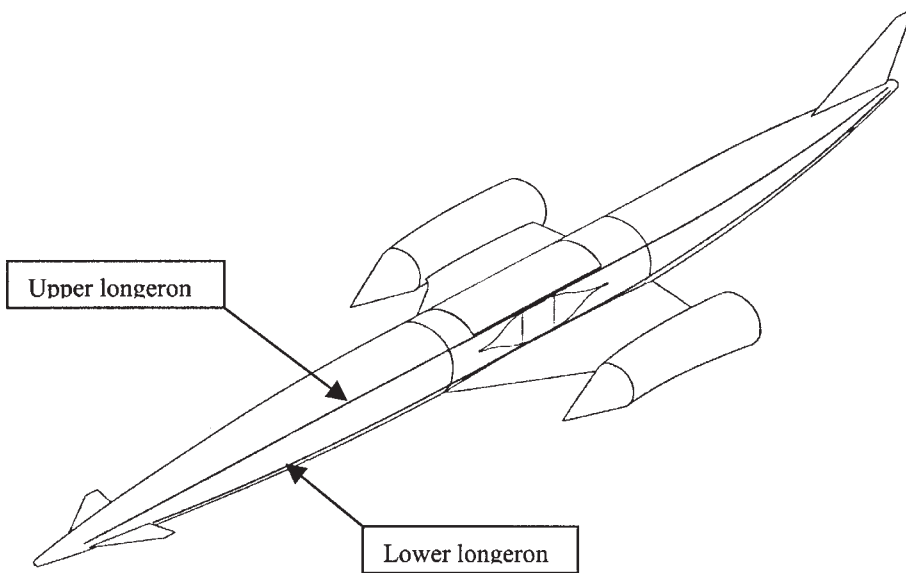
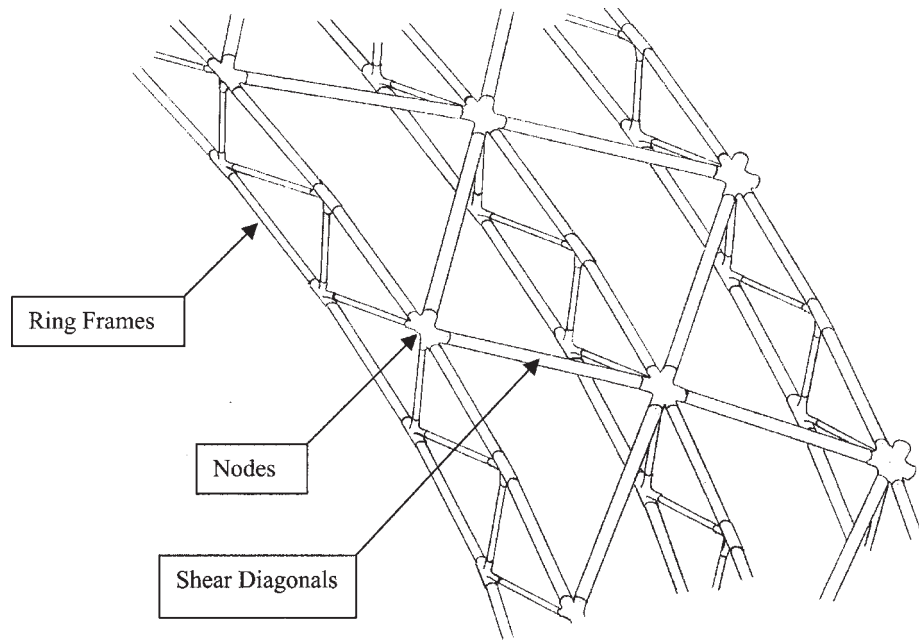


Fig. 4 Fuselage longerons.

minimise the structure mass, a material with the highest possible E/ρ is required which points to CFRP as the optimum, since the structure temperatures can be controlled within the material allowables. A further advantage of CFRP is that due to the predominantly on axis loading of the individual spaceframe struts, the full strength and stiffness of the fibres can be fully utilised.

Prior to fuelling the internal spaces of the vehicle are purged with dry nitrogen for safety reasons. During the ascent this nitrogen is gradually lost since the vehicle is vented to atmospheric static. Conversely during re-entry cooled and filtered air which has had water vapour removed is permitted to refill the internal spaces. Consequently the structure is always kept dry and resin matrix degradation associated with water absorption is avoided.

4. Fuselage Load Cases

For preliminary design purposes a set of load cases is required which are representative of the highest loads that the vehicle will be subject to in service. Identifying all of the potential abort conditions is a laborious task. However it is hoped that the following load cases encapsulate the highest loading, although not necessarily all the vehicle flight conditions that would contribute to the loading.

- 1) 1.9g pull-up manoeuvre plus 0.1g gust at Mach 5.4.
- 2) Takeoff abort, 4 m/s² emergency braking.
- 3) Both H₂ tanks depressurised but fully laden, 1.33g at Mach 0.5.
- 4) 1.25g manoeuvre plus 0.6g gust at Mach 0.6.
- 5) Max Fin lift 250kN plus load case 4.

- 6) Max cornering lateral 0.48g plus load case 2.
- 7) 2g, Mach 5.4, H₂ tanks pressurised (Payload bay frames)
1.25g, Mach 5.4, H₂ tanks depressurised (Tank frames)

Load case 1 corresponds to the hypersonic pull-up manoeuvre that the vehicle performs in order to reorient the trajectory for the rocket ascent. Load case 2 is a takeoff abort. Load case 3 represents an aborted fly-back condition with a depressurised but full tank plus modest manoeuvre 'g'. Case 4 corresponds to the worst combination of gust plus manoeuvre g that the vehicle is designed to withstand during the early subsonic phase of the ascent. The gust load factors are derived on the basis of a sharp edged vertical gust velocity of 12.2 m/s independent of altitude that equates to a probability of exceedance of 0.02% per flight. Case 5 is an attempt to represent the transient control loads needed to control an engine-out shortly after takeoff. Case 6

corresponds to the maximum oleo design sideload in conjunction with emergency braking and is roughly representative of a tyre blowout. Case 7 is used for frame sizing and represents the maximum aerodynamic crossflow loading attempting to distort the fuselage out of round.

Figures 5 and 6 show the variation in fuselage vertical shear force and bending moment for load cases 1 to 4. Comparison of the curves surprisingly reveals that it is the subsonic load case 4 that generates the highest loading for the majority of the fuselage length. This is predominantly due to the weight of the full hydrogen tanks cantilevered from the middle of the fuselage where it is supported by the wing. Conversely at higher Mach numbers the aft hydrogen tank empties and progressive forebody lift alleviates the front hydrogen tank bending moment. Figures 7, 8 and 9 illustrate the lateral shear force, bending moment and fuselage torque for load cases 5 and 6.

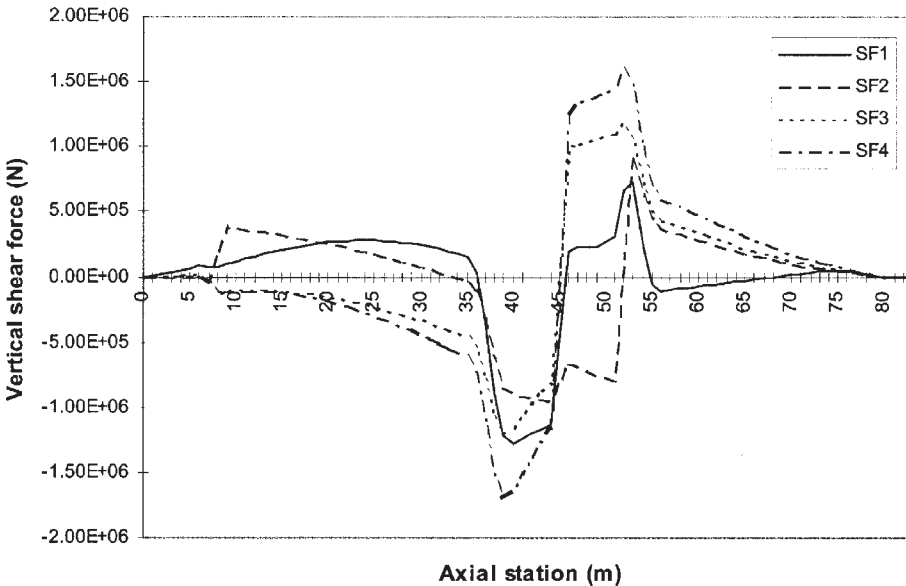


Fig. 5 Load cases 1-4: Vertical shear force distribution.

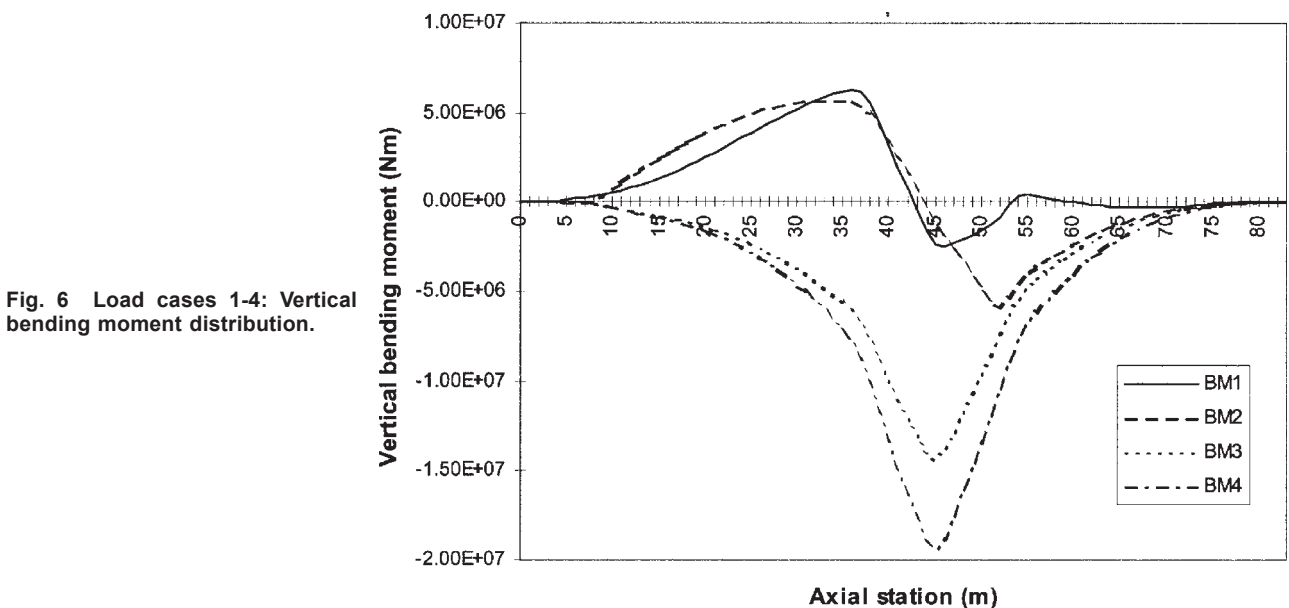


Fig. 6 Load cases 1-4: Vertical bending moment distribution.

Fig. 7 Load cases 5-6: Lateral shear force distribution.

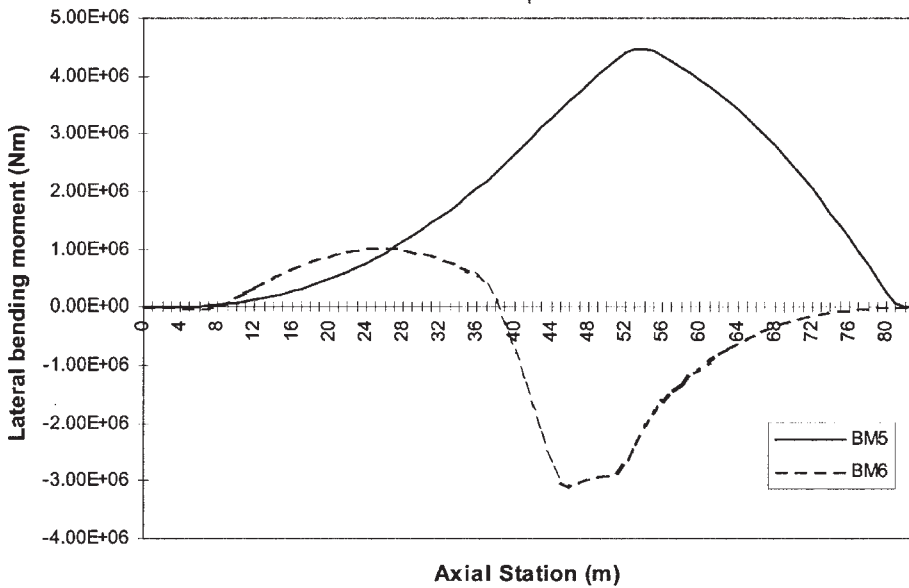
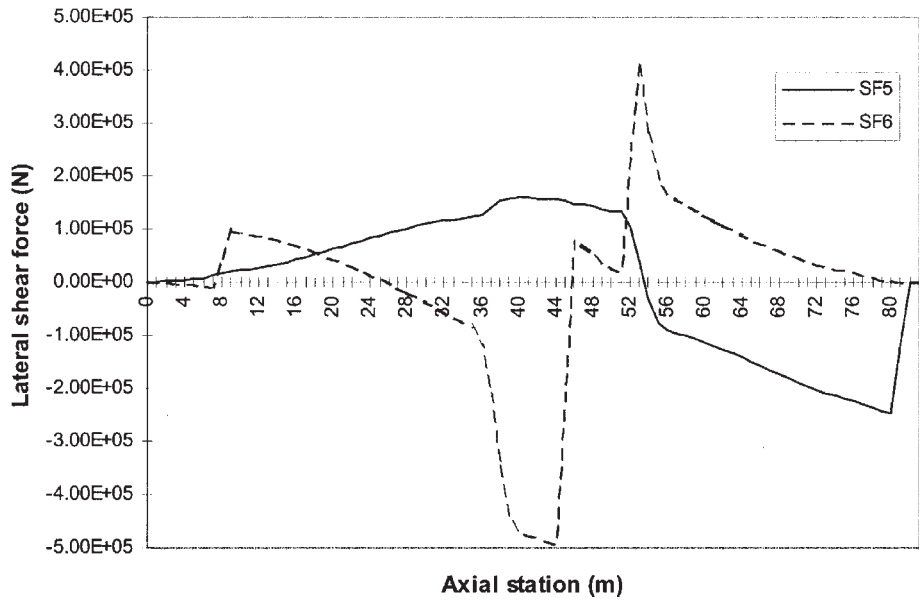
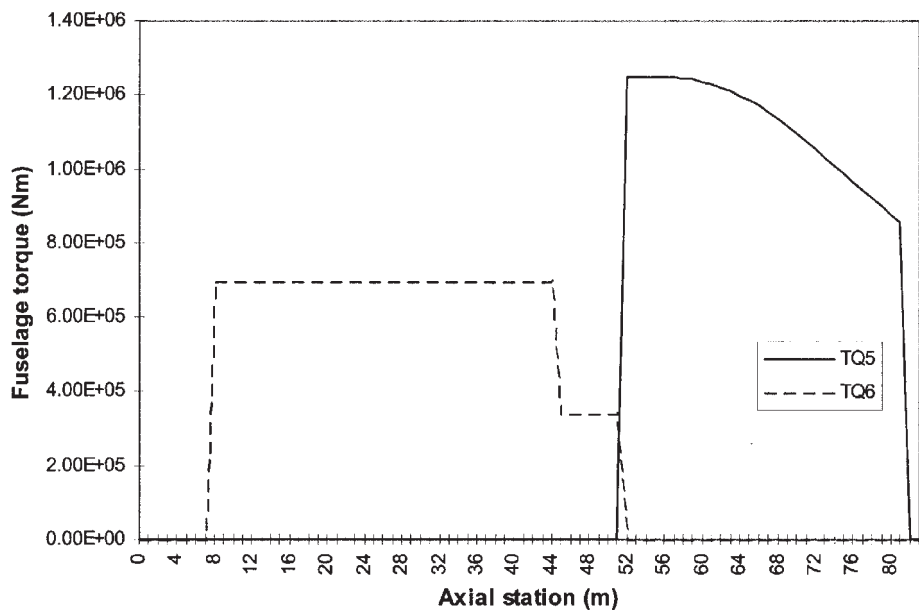


Fig. 8 Load cases 5-6: Lateral bending moment distribution.

Fig. 9 Load cases 5-6: Fuselage torque distribution.



5. CFRP Strut Design

The objective of the strut design is to determine the optimum fibre, radius, wall thickness and lay-up that give maximum allowable stress and hence minimum strut mass. For preliminary design purposes a safety factor of 1.5 was employed for both ultimate and buckling failure modes. Additionally, studies concentrated on the Toray 'J' series of carbon fibres due to their combination of high stiffness and strength (Table 1). When estimating the strut failure stress, consideration should be given to the ultimate tensile and compressive strengths of the laminate plus Euler and local wall buckling modes. Generally the strut design is aimed at maximising its compressive strength since the fibre tensile strength is roughly twice as high. The Euler and local wall buckling stresses were estimated by the methods outlined in Ref 3. Compared to an isotropic material the Euler buckling stress is adversely affected by the low shear modulus of the mostly unidirectional lay-up. Also it is very important to account for the non-linear stress/strain curve of carbon fibre reinforced plastic since at the compressive ultimate stress the tangent modulus is reduced to about 65% of its initial value. The local wall buckling stress is also lowered compared with an isotropic material due to the low modulus in the hoop direction. For this reason and for general handling strength hoop windings are incorporated into the bore and outside surface of the struts.

When considering a specific strut design a minimum gauge of 0.5 mm was assumed and then successive unidirectional plies of 0.125 mm were progressively added to determine the optimum wall thickness. Normally the optimum strut design is reached when the ultimate, Euler and local wall safety factors simultaneously correspond to the allowables. Depending on the applied load and strut length an optimum fibre exists which has the best balance between compression strength and modulus for Euler buckling resistance. For the SKYLON structure the modest loading and desire to limit the number of nodes resulted in the selection of relatively high modulus fibres that sacrificed strength in order to achieve higher stiffness.

6. Longerons

The fuselage is split into modular sections to facilitate assembly and maintenance. Consequently four joints are required in each longeron corresponding to the nosecone, forward tankage, centre fuselage, aft tankage and tailcone modules. The main

TABLE 1: Toray Unidirectional Carbon Fibre Reinforced Epoxy Properties.

Manufacturers' figures.

#2500-250°F cure epoxy, Vf = 60%.

Fibre type	E_T (GPa)	σ_T (MPa)	ϵ_T (%)	σ_C (MPa)
M35J	205	2450	1.1	1270
M40J	230	2450	1.1	1270
M46J	265	2210	0.8	1080
M50J	295	2010	0.7	980
M55J	340	2010	0.6	880
M60J	365	2010	0.6	785
X665	390	1910	0.5	740

hydrogen tankage is suspended on tangential ties from each longeron in a manner that locates the tankage concentrically whilst permitting radial and axial relative expansions. Since the tank and fuselage structure are tied together, bending deflections of the two components are forced to be nearly identical with the result that the tankage carries part of the overall fuselage bending moment and shear force. By maximising the load carrying contribution of the tankage the longeron mass is minimised. This effectively determines the fuselage bending strain at design loading conditions, since the maximum moment carrying capacity of the tank is reached when the imposed axial bending stress is equal to the nominal axial pressure stress (corresponding to the material strength limit on the tensile side and the onset of buckling on the compressive side). Allowing for the longeron distance from the neutral axis this condition corresponds to a maximum allowable longeron strain of $\pm 0.21\%$. Then to maximise longeron stress level and hence minimise mass, fibre selection is driven towards the maximum fibre modulus possible that does not exceed the fibre compressive strength limitations. This trade-off leads to the selection of M55J as the optimum fibre operating at a compressive stress level of 630 MPa, which equates to an ultimate compressive safety factor of 1.39.

It is worth noting that the aeroshell skin incorporates thermally compliant hairpins at every support and consequently cannot contribute to the overall strength or stiffness of the fuselage. Whilst this would appear to waste the potential structural contribution of the aeroshell it does have the advantage that the aeroshell does not impose a further more restrictive bending strain limitation. For preliminary design purposes the contribution of the truss shear diagonals to the overall bending strength has been ignored and consequently all of the applied fuselage bending moment is assumed to be carried by the longerons.

Figure 10 illustrates the minimum longeron cross sectional areas needed to meet the six design load cases. The actual longeron cross sectional areas are derived from the envelope of these curves. The total longeron mass not including joints or contingency is presently 583kg. The bending stiffness of the hydrogen tankage and the longerons is shown in fig. 11.

7. Frames

The aeroshell support pitch of 300 mm determines the ring frame spacing. The outer frame rail has the aeroshell support posts attached to it at 40 mm intervals and consequently has to withstand the local aeroshell pressure loading in bending. The frames are designed to resist the circumferential bending moment created by the aerodynamic crossflow over the fuselage. This bending moment varies around the fuselage circumference as well

as the frame axial station from the fuselage nose and the flight dynamic pressure and incidence. For SKYLON the bending moments peak at the high Mach number end of the airbreathing ascent since this corresponds to maximum vehicle incidence and forebody lift. Consequently the nosecone, tailcone and payload bay frames are designed to meet the 2g (normal) condition at Mach 5.4. However the frames that enclose the hydrogen tankage are designed differently. When pressurised the hydrogen tankage is able to carry the circumferential bending moments relatively easily, with a maximum radial deflection of only 52 mm at the 2g condition. The tank frames however are relatively shallow since they have to fit into the radial airgap and have a nominal section depth of only about 100 mm, and in addition have a very small radial clearance of 5 mm to the tank foam insulation. Consequently it is not practical to design the tank frames

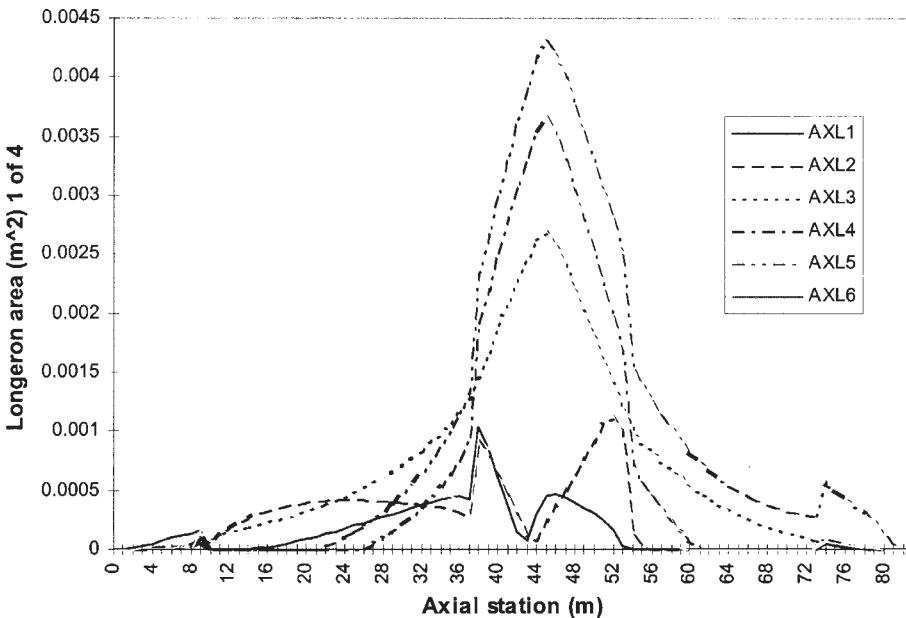
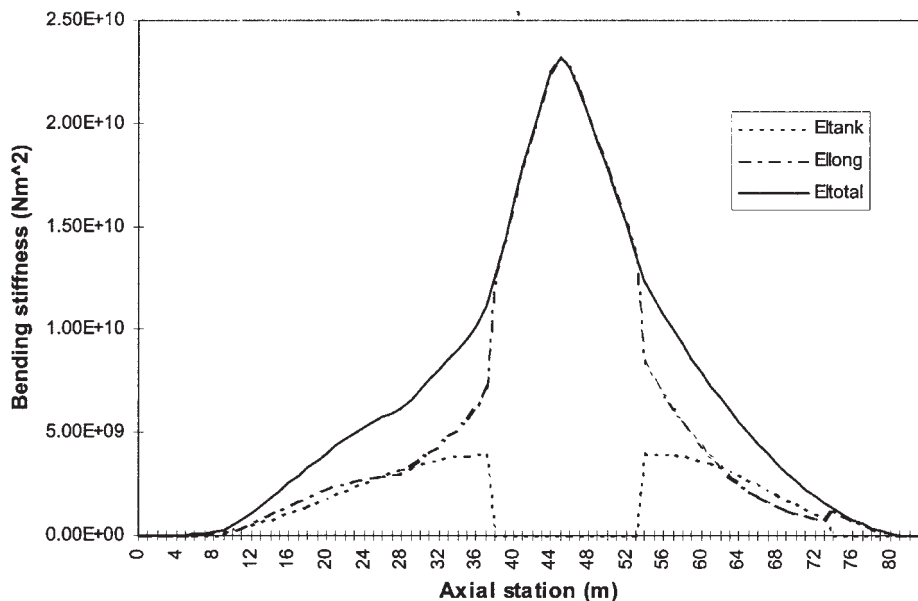


Fig. 10 Required longeron cross sectional areas.

Fig. 11 Fuselage bending stiffness distribution.



to carry all the moment without contacting the tank. Therefore under normal operating conditions the frames are designed to press up against pads on the tank surface thereby transferring the aerodynamic loading onto the tanks. Conversely in the event of a tank depressurisation the frames must be self-supporting but will be subject to a less severe abort manoeuvre assumed to be 1.25g at Mach 5.4.

For preliminary design purposes it was decided to design the frames with uniform strength around their perimeter despite the wide variation in applied bending moment. Investigation of the loading at various points down the fuselage resulted in a similar decision to maintain the frame rail cross sections constant along the fuselage but to increase the frame section depth to 250 mm in the payload bay area. Design investigation of the optimum truss geometry in conjunction with the shear diagonals eventually resulted in a decision to adopt a 300 mm node spacing. The optimum fibre to manufacture the frame rails that provides the best balance between modulus for Euler buckling resistance and compressive strength is M46J. The frame rails currently have a mean diameter of 18 mm, 5 plies of unidirectional prepreg giving a wall thickness of 0.625 mm and 10% by volume of ± 45 deg windings to provide the necessary shear strength for the aeroshell post loading. Under abort loading conditions the frame rails are subject to a direct stress of close to 700 MPa. The bare strut mass of the frame rails plus diagonals is 688 kg not including contingency.

Since the frames are only supported laterally at every other node it is anticipated that bracing wires will need to be attached to every unsupported node that is anchored to the 'fixed' nodes. A mass budget of 35 kg has been allocated to this structure based on 1 mm diameter Kevlar wires.

8. Shear Diagonals

The shear diagonals run in a zigzag pattern between each frame and carry the fuselage vertical and lateral shear loads in addition to torque loads from the fin and nosewheel (Fig. 4). Several alternative options are possible for the shear carrying structure including a combination of stringers with a single diagonal strut in each bay, or stringers with double diagonal tension wire. Preliminary investigation indicated little if any improvement for the alternative approaches although more detailed study is required to properly resolve the relative merits of each option including their effect on the node design and assembly.

The truss layout shown in fig. 4 evolved from an earlier design which consisted of frames joined by two layers of shear diagonals connected to the inner and outer frame rails, plus diagonals in the axial/radial plane. This initial layout was a perfect truss structure with each node fully supported in every direction. However ongoing design investigation revealed that the earlier layout would be relatively inefficient due to the effects of fuselage bending. Fuselage bending impresses an axial strain on the shear diagonals and consequently reduces the effective stress level able to resist the fuselage shear loading. To remain stable under the fuselage bending the shear diagonals required a minimum diameter of about 13 mm which grew to about 19 mm when the fuselage shear loading was included. Also at these strut diameters the wall thickness had to be increased to 0.75 mm to satisfy local wall buckling. Consequently it was decided to eliminate the inner layer of shear diagonals since by effectively combining the two layers the load per strut increased by only about 50% with the result that the total shear diagonal mass fell by about 33%. At the same time the opportunity was taken to replace the axial/radial diagonals with lightweight Kevlar tension ties whose stiffness was adequate to prevent toppling instability of the inner frame rail. Following further investigation it was realised that a basic conflict existed between the optimum node pitch needed to minimise the frame and shear diagonal masses when the shear diagonals were connected to every frame rail node. The frame rail mass reduced continuously as the node pitch was reduced. However the shear diagonal mass reduced as the node pitch increased until the struts were at an angle of about 45 degrees (due to the reduced fuselage bending strain component). Consequently it was decided to connect the shear diagonals to every other frame rail node which eased the conflict and resulted in the current arrangement. This change reduced the shear diagonal mass by a further 18%. A node pitch of 300 mm was picked since this minimises the total truss mass and results in a reasonable number of nodes.

The optimum fibre for the shear diagonals is M50J. Typically the struts have a diameter of 25 mm, wall thickness of 1.0 mm and operate at a stress level of about 650 MPa of which 215 MPa is due to fuselage bending. The required strut cross sectional areas needed to satisfy the six load cases are shown in fig. 12 whilst the actual structure employs areas derived from the envelope of these curves. The bare mass of shear diagonals is 736 kg not including contingency.

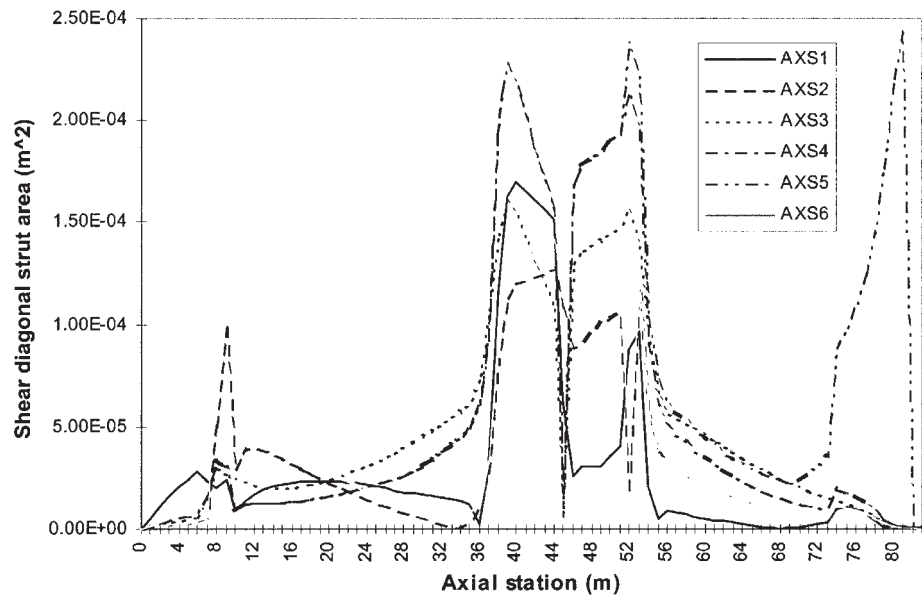


Fig. 12 Required shear diagonal cross sections.

9. Node Design

The nodes and the manner of joining them to the struts are generally regarded as the critical enabling technology for this type of structure. Although the majority of the loading is contained within the circumferential/axial plane, significant loading is also present in the radial direction due to the 'out of plane' struts. Also a large fraction of the nodes have to be split to enable final assembly of the truss structure. Consequently a 'pure' composite node appears impractical mainly due to the complex triaxial loading, but also due to the difficulty of effecting a lightweight joint that permits final assembly. Therefore metal nodes are currently favoured (either titanium or aluminium) due to their isotropic material properties and ability to form strong joints by welding operations. Titanium appears to offer more potential than aluminium due to its higher specific strength but also due to its ability to be formed into complex shapes by superplastic forming.

Each truss structure module will be initially assembled into four curved quadrants and then joined to the longerons to form the complete cylindrical truss. Due to the truss geometry it is not possible to insert all the struts into the tubular end joints without splitting most of the nodes. Therefore it is expected that axial 'strips' of truss structure would be preglued on jigs before flash butt welding the split nodes together to build up the quadrant in the circumferential direction (Fig. 13). Flash butt welding offers the potential of a near 100% weld efficiency without damaging the precured adhesive joints. Each node would be gripped in water cooled copper clamps to supply the electrical power which would also prevent the heat pulse conducting down the node limb into the tip of the adhesive joint.

The lap shear adhesive joint between the metallic node and the CFRP strut is dominated by the stress concentration at the ends. Scarfing both components to match the adherend stiffnesses appears to offer the best joint geometry although it is not possible to eliminate the stress concentration altogether due to the discontinuities at the joint edge. Further theoretical and experimental work is required to establish the best joint geometry taking account of the wide temperature range which the structure will be exposed to in the course of a mission, and also the practical constraints imposed by 'shopfloor' working conditions.

10. Fuselage Structure Mass Estimate

The final mass estimate for the SKYLON fuselage structure including a 15% contingency is shown in Table 2. The nodes represent about 33% of the total structure mass and consequently further work should explore ideas for reducing the node mass further. For simple 'rule of thumb' mass comparisons the CFRP fuselage structure is equivalent to an average area mass of 3.1 kg/m².

11. Strut Test Program

As part of a joint industry/university research program funded 50/50 by industry and the EPSRC, REL contributed 20 unidirectional CFRP struts 400 mm long with a bore diameter of 20 mm and nominal wall thickness of 0.75 mm comprised by 6 UD laminations of carbon/epoxy prepreg (fibre M46J/resin 737 Cycom). Each strut was fitted with two end nodes made of aluminium alloy (7075-T6) designed to match the stiffness of the CFRP and bonded with epoxy adhesive (3M's EC3448) via a scarfed axisymmetric joint. Seventeen of these struts were tested under

Fig. 13 Truss assembly dequence.

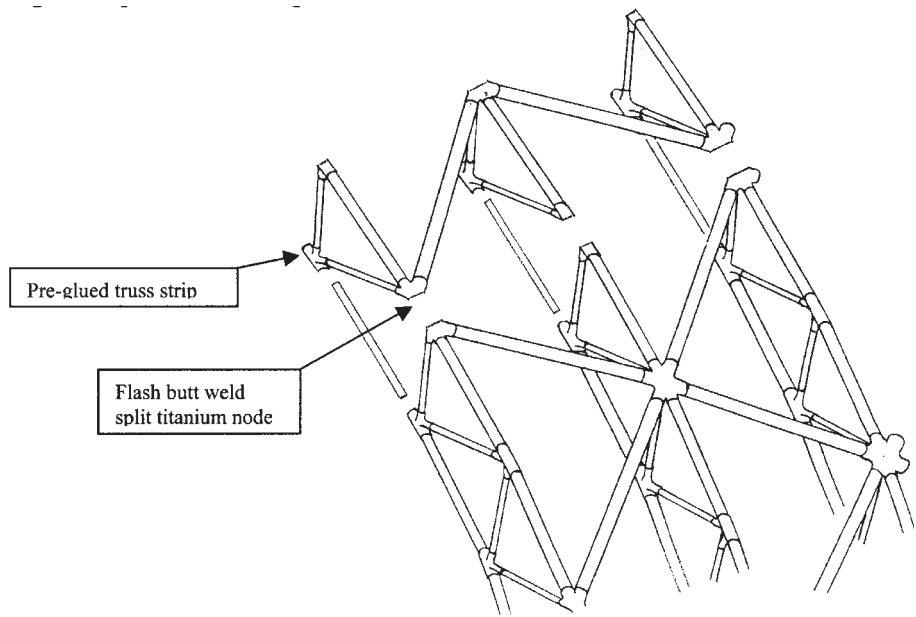


TABLE 2: C1 Fuselage Structure Mass Breakdown (Nov 1998).

Longerons	CFRP mass 583 kg (M55J fibre) x 1.15 contingency x 1.5 joints	1005 kg
Shear diagonals	CFRP struts 736 kg (M50J fibre) x 1.15 contingency x 1.5 nodes	1270 kg
Frame rails	CFRP struts 546 kg (M46J fibre) x 1.15 contingency x 1.4 nodes	879 kg
Frame diagonals	CFRP struts 142 kg (M60J fibre) x 1.15 contingency x 1.3 nodes	212 kg
Frame bracing wire	Kevlar ties 16 kg x 1.33 contingency x 1.5 nodes	35 kg
Miscellaneous items:	Wing carry through Local foreplane structure Local nose undercarriage structure Payload bay lining	573 kg
	Total	3974 kg

varying load conditions in order to verify the design methods and assess the strength of the bonded joint to the end node (Table 3).

11.1 Discussion of Tests and Results

RT and 80 °C Tensile tests

The tensile tests were finite element (FE) modelled in ALGOR using linear elastic elements. It was realised that this could only give an indication of the Tresca and shear stress distribution within the bonded region due to the simplistic material property assumptions. However it was predicted that the adhesive would reach a peak Tresca stress of about 150 MPa at the node tip at a load of approximately

42 kN and this was expected to be close to the failure condition of the adhesive. This is borne out by the test results in Table 3. It was expected that a larger variation in failure load would result from the misassembled specimens. The small change actually seen may reflect the benefits of the limited amount of yielding occurring in the adhesive.

The appearance of failed material in both the RT and 80 °C tensile tests indicates that a local crack is initiated by failure in the adhesive at the highly stressed region near the lip of the node sleeve, which then propagates all the way through the strut and the reinforcing carbon in a narrow region of the circumference. The load is then transferred from the broken fibres by shear into the neighbouring unfailed material resulting in shear failure and debonding of the remaining strut.

From the tensile tests it was concluded that the LFEM stress analysis gave a good indication of the strength of the joint, but also showed that the very peaked stress distribution was a bad feature, seriously degrading the load bearing capability of the joint to well below the promise of the constituent materials.

Low Temperature Tensile Tests and Fatigue Tests

These tests are discussed together because the appearance of the joint failure was, as far as could be determined, identical. The bond line of the adhesive to the scarfed CFRP strut failed by a clean fracture, resulting in the node coming off the strut. The very tip of the CFRP strut failed by tension and remained

TABLE 3: *Experimental Strut Testing Program.*

Test type	Strut identity Number	Failure load kN (cycles)	Comments	Failure mode
RT tension	1bu	44.0	longitudinal pre-crack	crack from node
	14cu	41.7		tip propagating through strut wall
	11cu	41.1	+2 mm axial error*	
	12cu	42.9	-2 mm axial error*	
80°C tension	18cu	42.0		as above
-100°C tension	19cu	11.3		fracture along bond to strut
	17cu	11.9		
RT fatigue (R=0.1)	6cu	33.4 (81)	80% ult. tensile	
	9cu	33.4 (394)	80% ult. tensile	fracture along bond to strut
	10cu	22.9 (6926)	55% ult. tensile	
	10cu	22.9 (13968)	55% ult. tensile	
	3bu (3bu)	15.0 (900,000) (42.0)	36% ult (no failure) tensile test of above	fracture along bond to strut
RT compression fixed ends	2bu	31.5		delamination near node
	4cu	29.8		
	16cu	35.4		
RT compression pin ended	7cu	16.9		Euler bucklingbreak near centre
	8cu	17.9		

Notes: The two letter post-script to the strut number indicates the testing institution; Cranfield University (cu) or University of Bristol (bu). * These two struts were deliberately manufactured with node displacement errors to assess tolerance to build errors.

inside the node and securely bonded. Strut No.3 which had survived 900,000 fatigue cycles and was then subsequently tensile tested, failed at 42.0 kN similar to the other tensile struts. But the failure mechanism was the same as for the other fatigue specimens and not from the high stress region at the tip of the node.

It was concluded that failure in these cases was by unstable propagation of defects at the bonded surface in fast fracture mode. At low temperature induced thermal stresses and poor fracture toughness working on the initially present defects were thought to be responsible for failure, while under fatigue conditions these initial defects were thought to grow to critical dimensions for failure to initiate in the prevailing stress field. More study is required to fully understand the micromechanics involved, but it is currently proposed that the defects are associated with the direct tensile stress at the end of each fibre where they break the surface of the strut and bond to the adhesive.

The rate of decrease in fatigue life with load was very similar to measurements made on two-dimensional lap shear joints during the course of this programme. The measured mean shear stress for the struts was however lower due to the highly peaked stress distribution in the adhesive that was worse than for the lap shear test pieces.

Fixed Ended Compression Tests

The manufacture of all of the struts left some misalignment of the ends relative to the strut axis. When gripped by the rigid jaws of the testing machine for fixed ended compression testing this induced some bending and shear force prior to the application of the loads. A detailed analysis showed that the maximum compressive stress was applied close to the edge of the node, which is where these test specimens failed. Calculation of the theoretical delamination stress levels agreed well with the test results on the assumption of approximately 2 to 3 % void volume at the interface of the individual laminates, introduced during manufacture. This is typical of such structures. The implied compressive strength of about 850 MPa is at the lower limit of what is required for the structure.

Pin Ended Strut Tests

The pin ended struts failed at very close to the expected Euler crippling load (15.8 kN) by buckling. The buckled struts carried substantial load until failure by compressive delamination occurred. The slightly 'higher than theory' measured crippling load is believed to be caused by the (unknown) stiffness of the Rose joints employed for the strut ends.

11.2 Summary of Test Results

The struts which have been tested so far have given

confidence that the design targets can be met. The simple tools for stress analysis (LFEM, classical buckling, composite micromechanics) give good predictions for the static strength of the struts.

The fatigue and low temperature results call for extensive redesign of the node joint, but have shown the nature of the problems and design work is in hand to avoid them. A search is now in progress for an adhesive with better fracture toughness characteristics at low temperatures, possibly at the expense of some static strength.

12. Conclusion

A novel structural concept has been proposed for the fuselage structure of the SKYLON spaceplane. This structure promises to be considerably lighter than alternatives and offers practical engineering advantages as well. A three year joint industry/academia research programme broadly confirmed initial estimates and found no fundamental technical drawbacks with the concept. Consequently Reaction Engines will continue to refine and develop this concept in the future.

References

1. R. Varvill and A Bond, "The SKYLON spaceplane", *JBIS*, **57**, pp.22-32, 2004.
2. "Innovative Approaches to Composite Structures" programme; Part of the EPSRC funded *Innovative Manufacturing Initiative*.
3. ESA, "Structural Materials Handbook Volume 1, Polymer Composites", European Space Research and Technology Centre, February 1994.

(Received 9 September 2003; 9 October 2003)

* * *